



Characterizing uncertainty in shear wave velocity profiles from the Italian seismic microzonation database

5 Federico Mori¹, Giuseppe Naso², Amerigo Mendicelli¹, Giancarlo Ciotoli¹, Chiara Varone¹, Massimiliano Moscatelli¹

¹C.N.R. – Istituto di Geologia Ambientale e Geoingegneria, Area della Ricerca di Roma 1- Montelibretti, Via Salaria km 29,300 - 00015 Monterotondo, RM, Italy

10 ²Dipartimento della Protezione Civile (DPC), via Vitorchiano 2, 00189 Rome, Italy

Correspondence to: Federico Mori (federico.mori@cnr.it)

Abstract. This research uses a large dataset from the Italian Seismic Microzonation Database, containing nearly 15,000 measured shear wave velocity (V_s) profiles across Italy, to investigate the uncertainties in seismic risk assessment. This extensive collection allows a detailed study of the seismic properties of soil with unparalleled precision. Our focus is on evaluating V_s variations with depth within uniformly clustered areas, known as seismic microzones. These zones are carefully identified based on their spatial correlation and homogeneity in geological, geophysical, and geotechnical characteristics, which are critical for accurate prediction of seismic response. We contrast these results with clusters formed purely based on geographic survey density (here defined geographic clusters), thereby assessing the depth of our understanding of the subsurface geological and geophysical context. These results were further compared with those reported in the seismic code and literature. This study of depth-dependent V_s variations helps to refine our models of subsurface seismic behaviour. Our main discoveries show that: 1) uncertainties associated with seismic microzones (geological and geophysical clusters) are consistently lower than those identified in geographic clusters, particularly in the first 30 m of depth; 2) V_s profile variations show negligible increases in uncertainty within a certain range of correlation distances (up to about 4,500 m); 3) uncertainties for seismic microzones are lower than those previously reported in seismic codes and in the literature, indicating the effectiveness and precision of our methodological approach. The results of this study significantly improve local seismic response analysis and highlight the critical role of depth and spatial correlation in understanding seismic hazard. The dataset is available at <https://doi.org/10.5281/zenodo.10885590> (Mori et al., 2024).

1 Introduction

A seismic microzonation project has been active in Italy since 2009 for the most vulnerable Italian municipalities, about 4,000 out of approximately 8,000 (Moscatelli et al., 2020). This project is based on the ability to map homogeneous zones with respect to the expected amplification of seismic ground motions (so-called Seismic Microzones, hereafter SM). These zones



must be sufficiently detailed to account for local features that influence ground motion and to identify earthquake-induced ground instabilities (e.g., liquefaction, landslides, surface faulting, soil compaction).

All the data collected in the Italian seismic microzonation project, both geographical (e.g., shapes of the SM and location of the surveys) and alphanumeric (geological, geotechnical, and geophysical parameters) were standardised according to the Seismic Microzonation Working Group (2008) and stored in a database. The results of the seismic microzonation studies are freely available at the link: <https://www.webms.it/servizi/stats.php> (last access: March 2024). The database has proved its great potential over the years: it has been crucial for the development of the methodology used to produce the Vs30 (Mori et al., 2020), and the seismic amplification factor maps of Italy (Falcone et al., 2021). Gaudiosi et al. (2023) recently published a collection of shear modulus reduction and damping ratio curves primarily derived mainly from the database, while Varone et al. (2023) benefited from this dataset in assessing earthquake-induced liquefaction in Northern Italy. Shear wave velocity (Vs) profiles obtained from geophysical prospecting are a highly valuable component, along with other data. The collection contains over 23,500 Vs profiles, last updated in December 2022, evenly distributed throughout Italy.

Researchers have extensively investigated the variation of Vs with depth over time. Stewart et al. (2014) used the Savannah River dataset to examine the variations of Vs at various depths, building on previous work by Toro (1997). The suggested standard deviation for the natural logarithm of Vs ($\sigma_{\ln V_s}$) is 0.15 for depths up to 50 m and 0.22 for depths beyond 50 m. In parallel, the US nuclear industry developed the SPID (Screening, Prioritization, and Implementation Details in EPRI-SPID, 1993) framework, which recommends $\sigma_{\ln V_s}$ ranging of 0.25 for the first 15 m and 0.15 for greater depths, again depending on the amount of available data. Shi and Asimaki (2018) and Toro (1995, 2022) studied the detailed uncertainty in Vs profile datasets with the aim of proposing several randomisation models. Romagnoli et al. (2022) performed a statistical analysis on about 3,500 Vs profiles within the Italian territory to evaluate the variability of Vs values in the engineering geological units of the subsurface, as outlined in the seismic microzonation studies by Seismic Microzonation Working Group (2008).

The results of previous studies show an apparent complexity in the spatial structure of the Vs parameter and divergent trends in its uncertainty with depth, highlighting the need for further investigation in this area. Following these studies, the present work uses the considerable amount of information available from the Italian seismic microzonation database to determine the uncertainty associated with the variability of Vs with depth. In particular, the vertical profiles of $\sigma_{\ln V_s}$ are calculated and presented.

As a by-product, this work also provides for the first time the largest database of Vs profiles (about 15,000 refined profiles out of approximately 23,500 available) ever distributed worldwide, derived exclusively from geophysical surveys (see Mori et al., 2024, <https://doi.org/10.5281/zenodo.10885590>). The flow chart in Fig. 1 highlights the steps followed in this study to calculate the $\sigma_{\ln V_s}$ values of the Vs profiles from the Italian seismic microzonation database. The steps can be summarised as follows:

1. build a robust and reliable **dataset of Vs profiles** by removing any errors or duplicates (section 2.1);
2. define the **range values** in the **spatial correlation analysis** between the Vs profiles surveys (sections 2.2 and 3.1);
3. check the distribution pattern of the data (i.e., **clustering**) using Moran's Index (sections 2.3 and 3.1);



- 65 4. define **geographic density-based clusters (GC)**, HDBSCAN method, sections 2.3 and 3.1) and **geological-geophysical based clusters (SM)**, seismic microzonation studies, sections 2.3 and 3.1);
5. calculate the $\sigma \ln V_s$ of clusters formed by means of range value and GC (section 3.2);
6. calculate the $\sigma \ln V_s$ of clusters defined by means of range value and SM (section 3.2);
7. compare the results obtained from the two clustering methods and determine the approach that provides **lower $\sigma \ln V_s$ values** (section 3.2);
- 70 8. compare the obtained lower $\sigma \ln V_s$ values with those implemented in **seismic codes or reported in existing literature** (section 3.3).

The results demonstrate the effectiveness of the analysis performed on SM clusters: the standard deviation values of these clusters are significantly lower for all depths examined. These results are crucial for improving the randomisation of V_s profiles in numerical simulation codes used for surface seismic response calculations and hazard analysis.

75

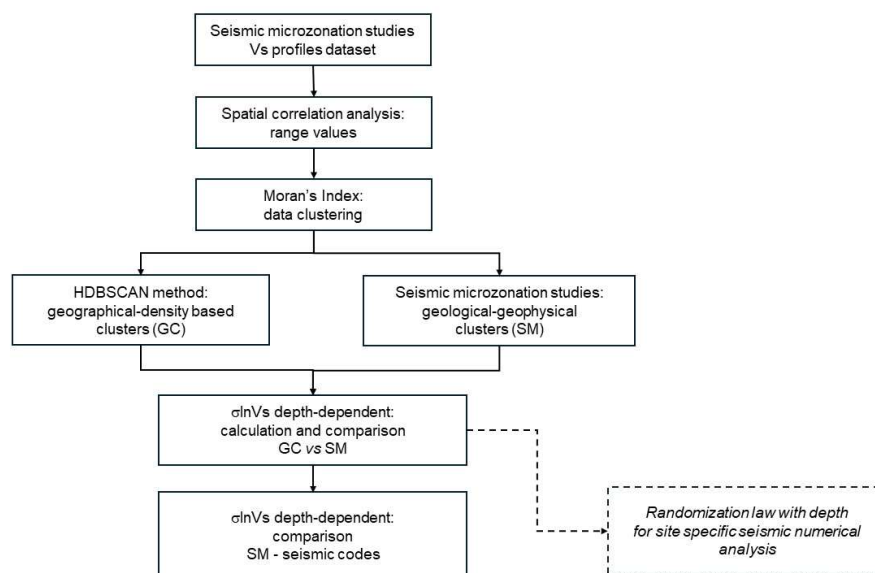


Figure 1: Flow chart describing the steps described in the paper to define the $\sigma \ln V_s$ (standard deviation of V_s natural logarithm) depth-dependent values of the V_s profiles.

80 2 Data and Methods

2.1 V_s profiles dataset

The original V_s database includes 23,512 V_s investigations classified as either punctual or linear. These investigations include Down-Hole (DH), Cross-Hole (CH), Extended Spatial Autocorrelation - Spatial Autocorrelation Phase Analysis (ESAC-SPAC), Multichannel Analysis of Surface Waves (MASW), Spectral Analysis of Surface Waves (SASW), Refraction



85 Microtremor (REMI), Seismic Refraction (SR), and Frequency-Time Analysis (FTAN). Table 1 shows a detailed analysis of the number of investigations by type and their corresponding geometries. All linear investigations are referenced to their center points to maintain consistency in data format.

Geometry	Type of investigation	Count	%
Point	DH	1,091	7.3
Point	CH	12	0.1
Point	ESAC-SPAC	753	5.1
Line	MASW	9,457	63.5
Line	REMI	3,160	21.2
Line	SASW	23	0.2
Line	SR	190	1.3
Line	FTAN	211	1.4

Table 1: Breakdown of the number of Vs investigations for type and geometry.

90

The dataset was refined by selecting investigations that reached a minimum depth of 30 meters and by removing outliers based on the interquartile range criterion applied to the natural logarithm of the Vs30 value. This filtering approach provided a refined dataset of 14,897 investigations (see supplementary material). The Vs profiles were discretized with a depth step size of 1 m. The obtained profiles include Vs values ranging from 75 to 2,034 m/s, with depths varying from 1 to 120 m (Fig. 2). The hexbin plot, along with the marginal histograms, effectively displays the dataset by showing the frequency of Vs-depth pairs on a logarithmic scale, after removing outliers based on the interquartile range criterion applied to the natural logarithm of the Vs30 value (Fig. 2). The histograms provide a detailed overview of the distribution of Vs values and depths, independently.

95

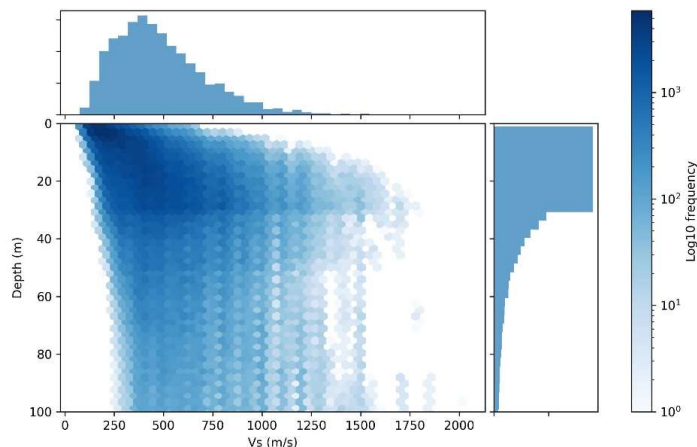
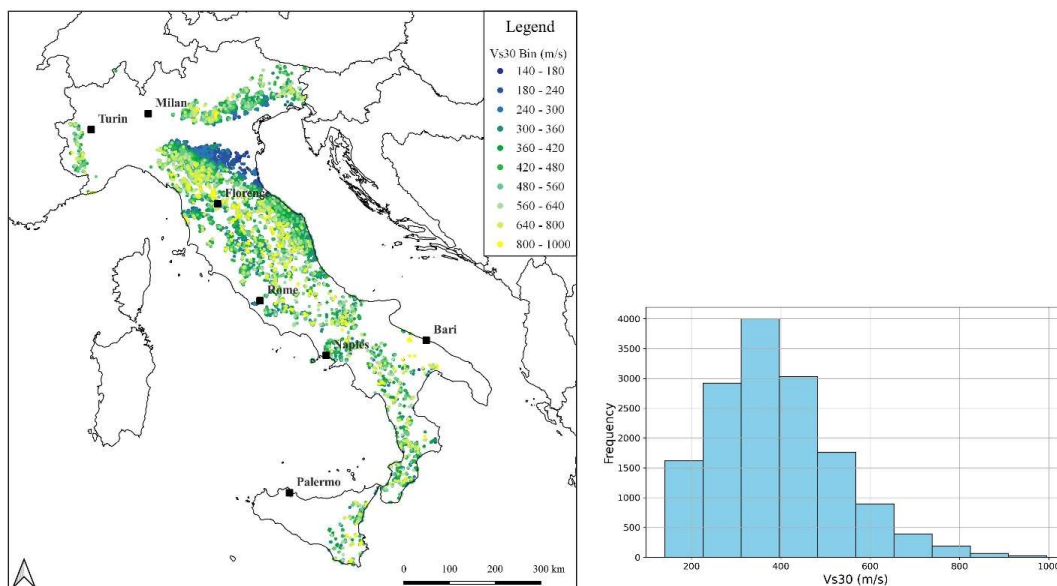


Figure 2: Hexbin heatmap of Vs, and depth and frequency distribution of Vs values (top) and of depths (right).



100 The spatial distribution of Vs30 values across Italy for the refined 14,897 Vs profiles is reported in Figure 3 left. The highest values of Vs30 are distributed in the mountain ranges while the lowest values are concentrated in the central-eastern region of the Po Valley.



105 **Figure 3: Left - geographic distribution of the refined 14,897 Vs profiles across Italy in terms of Vs30; Right - frequency distribution of Vs30.**

The latter information will be useful in discussing some of the results obtained. Furthermore, focusing on the frequency of these values, Figure 3 right shows that they are lognormally distributed.

110 2.2 Spatial correlation analysis

Experimental variograms were used to examine the spatial structure, such as autocorrelation, of the Vs data in terms of distance and variability.

The experimental variogram is a fundamental tool used in spatial statistics to quantify the spatial autocorrelation of regionalized variables, such as temperature, precipitation, or soil properties, across geographic space (Journel and Huijbregts, 1978; Deutsch and Journel, 1998; Chiles and Delfiner, 2009). It provides insight into the relationship between the values of a variable based on distance or direction. The variogram quantifies the dissimilarity between pairs of observations at different locations based on their geographical separation. It describes the spatial relationship structure of the variable under study. The variogram function [1] is commonly referred to as $\gamma(h)$, where h represents the lag distance or separation between two locations.

The formula for the experimental (semi)variogram $\gamma(h)$ can be expressed as Eq 1:

120



$$\gamma(h) = \frac{1}{2N(h)} \sum_{i=1}^{N(h)} [Z(x_i + h) - Z(x_i)]^2 \quad (1)$$

where, $N(h)$ represents the number of pairs of observations separated by the lag distance h , $Z(x_i)$ denotes the value of the variable at location x_i , and $Z(x_i+h)$ is the value of the variable at a location h units away from x_i . The sum is taken over all pairs of observations separated by the lag distance h .

The experimental semivariogram is typically computed by first dividing the study area into a set of lag intervals. For each lag interval, the average squared difference in values between pairs of observations separated by the corresponding lag distance is calculated. This process is repeated for multiple lag intervals, resulting in a curve representing the variogram function. For sample points at close distances, the difference in values between points tends to be small. In other words, the semi-variance is small. But when the sample points are further apart, they are less likely to be similar. This means that the semi-variance becomes large. As the distance from the sample points increases, there is no longer a relationship between the sample points. Their variance begins to flatten out, and the sample values are not related each other.

According to this spatial behaviour, the variogram curve typically exhibits three common descriptors and distinct parameters: i) the nugget (C_0), ii) the sill ($C-C_0$), and iii) the range (a) (Fig. 4).

The nugget (C_0): Theoretically, at zero separation distance (lag =0), the variogram value is 0. However, at an infinitesimally small separation distance, the variogram often exhibits a nugget effect, which is a value greater than 0. The nugget effect is a phenomenon present in many regionalized variables and represents short-scale randomness or noise in the regionalized variable typically caused by measurement error or micro-scale variability. It can be seen graphically in the variogram plot as a discontinuity at the origin of the function.

The sill ($C-C_0$): This is generally considered to be the variogram value at which the variogram curve flattens with increasing distance. The sill is also considered to be the variance of the data entering the variogram calculation. The sill (C) represents the plateau of spatial dependence and indicates the maximum achievable spatial correlation.

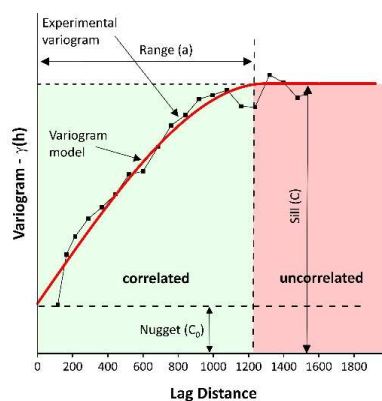


Figure 4: Theoretical experimental semivariogram and model with corresponding parameters. For details, see text.



145 The range (a) This parameter indicates the distance beyond which spatial correlation is negligible. Sample locations separated
by distances closer than the range are spatially autocorrelated, whereas locations further apart than the range are not.
It can be evaluated valuable insight into the spatial structure and variability of regionalized variables by analysing the shape
and parameters of the experimental variogram. The experimental variogram is usually fitted by a simple function (variogram
model) using a mathematical formula whose main parameters (i.e. sill, range and nugget) are used to calculate values for
150 unsampled locations using the kriging technique (Goovaerts, 1997; Isaaks and Mohan Srivastava, 1989; Journel, 1987; Krige,
1966; Matheron, 1971;).

2.3 Dataset Vs profiles clustering

After the quantification of the spatial correlation between the Vs surveys, we checked whether the same surveys were clustered.
155 For this verification, we used the Moran's Index. Moran's Index quantifies spatial autocorrelation by considering both the
locations and attributes of features simultaneously, and evaluates the distribution pattern (i.e., points or polygons) based on a
set of features and their associated attribute by comparing the study pattern with standard clustered, dispersed, or random
patterns. We used the Spatial Autocorrelation tool in ArcGIS Pro (ESRI.com). The programme calculates the Moran's I index
value and provides a z-score and p-value to assess the importance of the index. P-values are numerical estimates of the area
160 under a given distribution curve, determined by the test statistic.

After checking whether the surveys in the dataset were clustered, we used two clustering methods. The first method involves
a geographical analysis (i.e., location of the survey points) to define geographical clusters (GCs), while the second method is
to consider SM polygons as clusters (SMs), extracted directly from the seismic microzonation projects.

165 *Geographic clustering: HDBSCAN method*

Geographical clustering considers the geographical location of the Vs surveys, and therefore the density of survey points in a
given area, without reference to the Vs parameters. The clustering was performed using the algorithm HDBSCAN
(Hierarchical Density-Based Spatial Clustering of Applications with Noise in McInnes et al., 2017) algorithm available in
ArcGIS Pro 3.2.2 suite (Copyright© 2023, Esri. Inc.). HDBSCAN is a density-based clustering method that, thanks to the
170 concept of mutual reachability distance, is particularly able to manage issues related to the recognition of clusters with different
densities. The process begins with the construction of a minimum spanning tree that incorporates this mutual reachability
distance, followed by the development of a hierarchical tree of clusters. This methodological foundation allows the adaptive
identification of clusters without the need for a predefined number of clusters, thus providing deeper insights into the intrinsic
structures of data by combining density-based clustering with hierarchical analysis and stability metrics.

175

Geological-geophysical clustering: seismic microzonation studies

Another method of clustering Vs profiles involves the use of the boundaries of SM polygons (Figure 5). As mentioned in the
introduction, the seismic microzonation project that is underway in Italy involves the identification of SMs, that are several



square kilometres in size, homogeneous in terms of expected seismic amplification, and defined by means of geological,
180 geotechnical, and geophysical information.

The 14,897 Vs profiles provided are associated with 7,583 SMs distributed throughout the Italian territory (updated to
December 2022). These SMs are characterized by a variable number of Vs profiles, ranging from 1 to several tens. In order to
assess the statistical significance of our classification, a spatial statistical analysis of the Vs profile within the SMs was
performed. For statistical purpose only, 1,271 SMs containing at least 3 investigations were considered, giving a total of 7,350
185 Vs profiles. Most of the selected SMs (about 900) are characterised by 3 to 5 Vs profiles, while a few SMs contain more than
25 Vs profiles with a maximum of 68 investigations.

A SM is typically characterized by an extent of up to 20 km² with an interquartile range of 6 km² and a median value of 4
km², while the Euclidean distance between the Vs profiles within individual SMs mainly ranges between few metres and 5.5
km, with a median value of 1.8 km and interquartile range of 1.5 km.

190

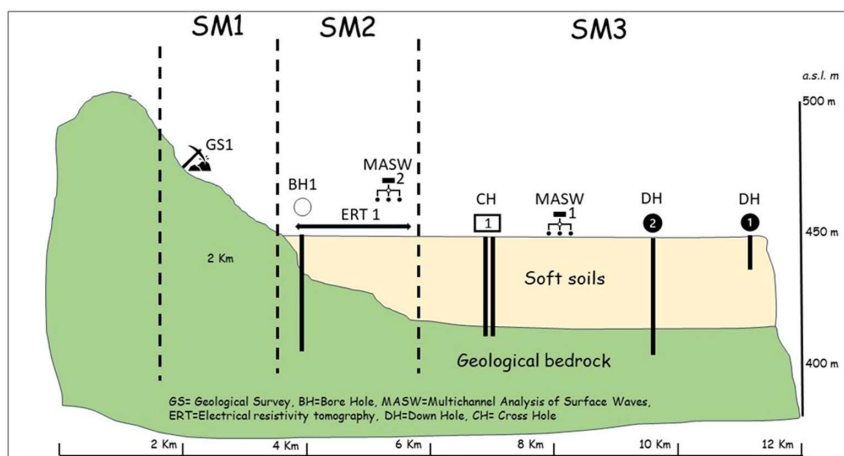


Figure 5: Example of a geological profile showing the partition into three Seismic Microzones (SM), identified by means of the geological information and the results of geotechnical and geophysical investigations. The drawing is not to scale.

195 3 Results

3.1 Definition of range value and clustering

The experimental variograms of the three Vs synthetic measurements Vs10, Vs20, and Vs30 show a spatial structure fitted by
nested (spherical + exponential) semivariogram models (Fig. 6). The first spatial structure shows a range of about 4,500 m,
while the second structure shows a range of 25,000 m. Table 2 shows the semivariogram parameters of the three models for
200 the three analyzed Vs synthetic measurements.

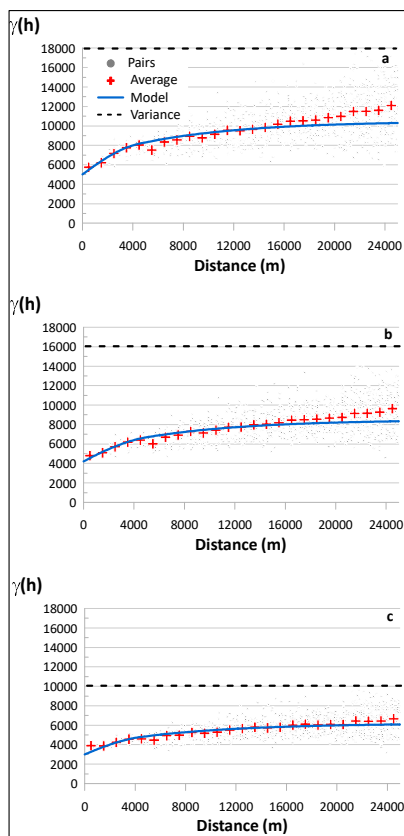


Figure 6: Experimental semivariograms and nested models for a) Vs30, b) Vs20, and c) Vs10

Parameter	Nugget	Model 1	Range 1	Sill 1	Model 2	Range 2	Sill 2	Total Variance	Nugget/ Variance
Vs30	5000	Sph	4500	1500	Exp	25000	4000	18000	0.28
Vs20	4200	Sph	5000	1000	Exp	25000	3300	16000	0.26
Vs10	3000	Sph	4500	800	Exp	25000	2400	10000	0.32

Table 2: Semivariogram parameters of the nested models (spherical + exponential) for the three Vs synthetic measures analyzed: Vs30, Vs20, Vs10.

205

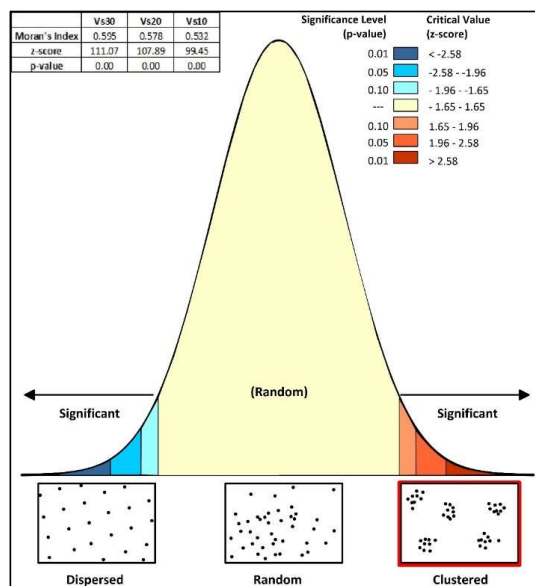
It is useful to emphasize that our results are comparable with those results of Zhou et al. (2023), who carried out a quantitative study analyzing the lateral variation of the Vs profile and Vs30 in plain and piedmont terrains at short distances ranging from hundreds of metres to several kilometres. Even in their study, the variation in site conditions does not significantly increase with distance within a specific range, usually between 1 km to 3-5 km.

210

The Morans' Index was calculated for the three synthetic parameters Vs30, Vs20, and Vs10, corresponding to the average of Vs in the first 30, 20, and 10 metres, respectively.



The results (Fig. 7) show a strong trend towards clustering of the data, so we applied the two clustering methods described in Method section.



215

Figure 7: Report of the Moran's Index (spatial autocorrelation) statistic showing that the pattern was clustered. p-Value: probability; z-score: standard deviation. for: a) Vs30, b) Vs20, c) Vs10

The range value of 4,500 m of the first spatial structure was then used to filter clusters for both GC and SM, to obtain a high-quality dataset for assessing the variability of Vs.

220

Table 3 shows the effect on the number of Vs profiles and clusters after applying two filters: minimum number of surveys in the cluster (i.e. 3) and spatial correlation distance (i.e., range value 4,500 m). The number of clusters obtained for the two methods (Tab. 3) is comparable (1759 vs. 1120 for GC and SM, respectively) and they are used to perform the final statistics on our target $\sigma_{ln}Vs$.

225

	Geographic clustering		Seismic microzonation	
	before filters	after filters	before filters	after filters
Vs profiles (n.)	12480	9601	14897	5561
Clusters (n.)	1977	1759	7583	1120

Tab. 3: Number of Vs profiles and number of clusters obtained after applying the two filters: minimum number of surveys (i.e. 3) and spatial correlation distance (i.e., range value 4,500 m).



230 Figure 8 shows the results of the distance distribution between Vs profiles after filtering with 3 minimum surveys and a range value of 4,500 m: statistics are comparable (median values 500 m and 700 m for SM and GC clustering, respectively).

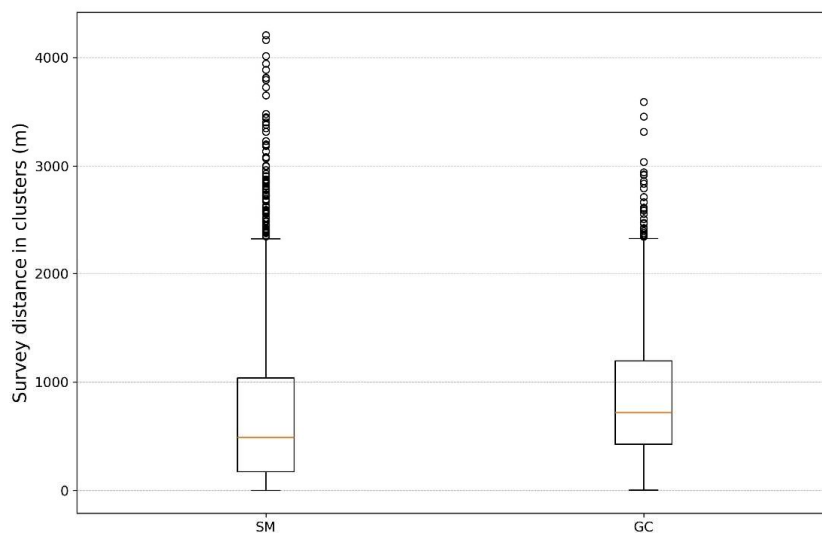


Fig. 8: Distances distribution between Vs profiles after filtering with 3 minimum surveys and 4,500 m range value.

235 3.2 $\sigma \ln V_s$ statistics in SM and GC clusters

After filtering the SM and GC clusters with the number of surveys and the range value of the first variogram structure, we calculated the uncertainties as a function of depth. Uncertainty models assume that Vs values at each depth follow a lognormal distribution (Toro, 2022 and references therein), therefore the uncertainties are determined by calculating the $\sigma \ln V_s$.

Considering both SM and GC clustering, for the Vs profiles associated with the clusters:

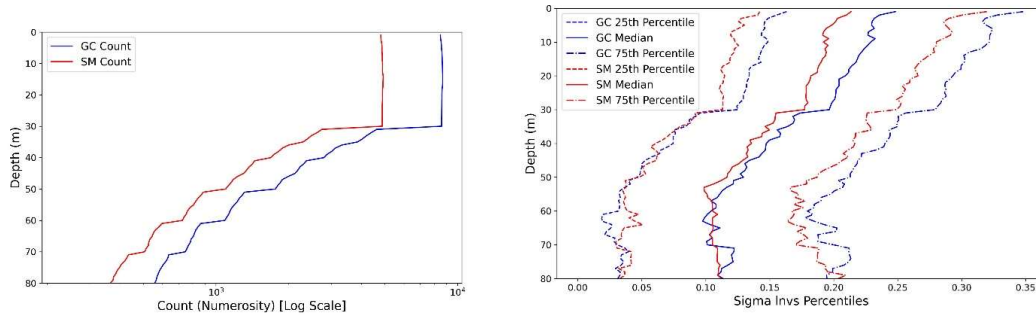
- 240
- the $\sigma \ln V_s$ value was obtained for each meter of depth (Fig. 9 left)
 - the percentiles 25th, 50th, 75th of $\sigma \ln V_s$ were obtained for each meter of depth (Fig. 9 right).

The general trend of the curve in Figure 9 right, especially that of the 50th percentile, reflects a trend already known and often reported in the literature (Toro, 2022 and references therein): shallower layers show greater variability and larger $\sigma \ln V_s$ values, while Vs values remain almost constant below a depth of 50 m. The most interesting results are in the absolute $\sigma \ln V_s$ values:

245 the 50th percentile curve never exceeds the value of 0.21 and at depth below 50 m is about 0.11. Figure 9 right also shows comparison between $\sigma \ln V_s$ values of SM clusters (red lines) and GC clusters (blue lines); it clearly shows the better



performance of SM for clustering the $\sigma \ln V_s$ values, which are always higher in the GCs, although the trend of the curve is very similar.



250 **Figure 9: Left - The numerosity of data per meter: very large for both methods, with a slight prevalence for GC method. The same figure shows that at about 30 m depth there is a variation in the number of data because many of the surveys do not investigate depths beyond 30 m; Right - $\sigma \ln V_s$ statistics: comparison among $\sigma \ln V_s$ values of SM and GC clustering (25th,50th,75th percentile).**

The difference between the uncertainty values in percent for the two methods is calculated by the following Eq. (2):

255

$$\text{Percentage Variation} = [(\sigma \ln V_{s_SM} - \sigma \ln V_{s_GC}) / \sigma \ln V_{s_SM}] * 100 \quad (2)$$

Where:

- $\sigma \ln(V_{s_SM})$ is the standard deviation of the natural logarithm of the measurement obtained with the SM clustering.
- $\sigma \ln(V_{s_GC})$ is the standard deviation of the natural logarithm of the measurement obtained with the GC clustering.

260

In general, there is a 14% decrease in favour of the SM method within the first 30 m, followed by a 9% reduction from 30 to 50 m, and a 4% decrease from 50 to 80 m. The decrease in the first 30 m, represents the quantification of the importance of geological and geophysical information in reducing uncertainties. Below 30 m, the difference in uncertainty between the two methods decreases to about 9% and then to 4%, due to the greater homogeneity of geological and geophysical properties at greater depths.

265

3.3 Comparison with seismic code and literature uncertainties

We also compared our results with the uncertainties implemented in seismic codes and with known literature data (Figs. 10 and 11). Appendix B of the EPRI-SPID (1993) provides guidance on the development of site response, including the quantification of uncertainty. In cases where limited site response data are available, EPRI-SPID (1993) recommendations define aleatory uncertainty as lateral variations within a footprint of approximately 100 to 200 m. The EPRI-SPID (1993, Section B-4.1) recommends $\sigma \ln V_s$ values of 0.25 at the surface, decreasing to 0.15 at 15 m and deeper. Figure 10 shows the comparison of these values with the results obtained in the SM clusters also including the site-specific values from Toro (1995,

270



1997, 2022). The plot (Fig. 10) shows a clear improvement for the first 10-15 m, but in general all values of the depth
275 uncertainties from EPRI-SPID (1993) and Toro (1995,1997, 2022) are within the 25th and 75th percentiles of our results.
In earthquake-resistant standards (i.e., European EC8, NEHRP for the USA, and Italian NTC18), the dynamic characterisation
of sites is represented by the synthetic value of V_s30 . The Toro (1995) model is also developed for 4 NEHRP V_s -based soil
classes (B: $V_s30 > 760$ to 1500, C: 360 to 760, D: 180 to 360, E: < 180). Figure 11 shows $\sigma \ln V_s$ of V_s profiles from our high-
280 quality dataset, reclassified according to the 4 NEHRP soil categories and considering a minimum number of 150 values for
each metre depth. Values of $\sigma \ln V_s$ constant with depth according to Toro (1995) are also shown in Figure 11 for reference.
The following observations can be made.

- For soil category B (soil category A in the Italian building code), there is a strong variation with depth. This tendency
is due to the strong heterogeneity of the rocks at the surface due to fracturing and weathering and, conversely, to the
homogeneity of the rocks at greater depths.
- For soil categories C and D, the $\sigma \ln V_s$ values are fairly constant but generally larger to those obtained by SM
285 clustering.
- For soil category E, the $\sigma \ln V_s$ values are low and comparable with those obtained by SM clustering (see Fig. 11).
Considering that almost all the sites with these V_s30 values are located in the central eastern part of the Po Valley
(Fig. 3), this is not surprising. The plot of uncertainties for soil category E somewhat describes a regional cluster, that
290 is much larger than an SM cluster but contains sites with similar V_s profiles.

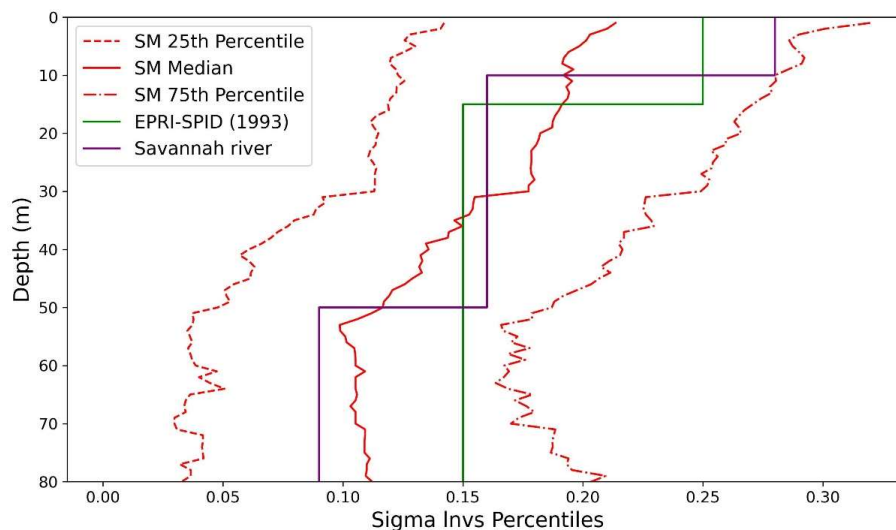
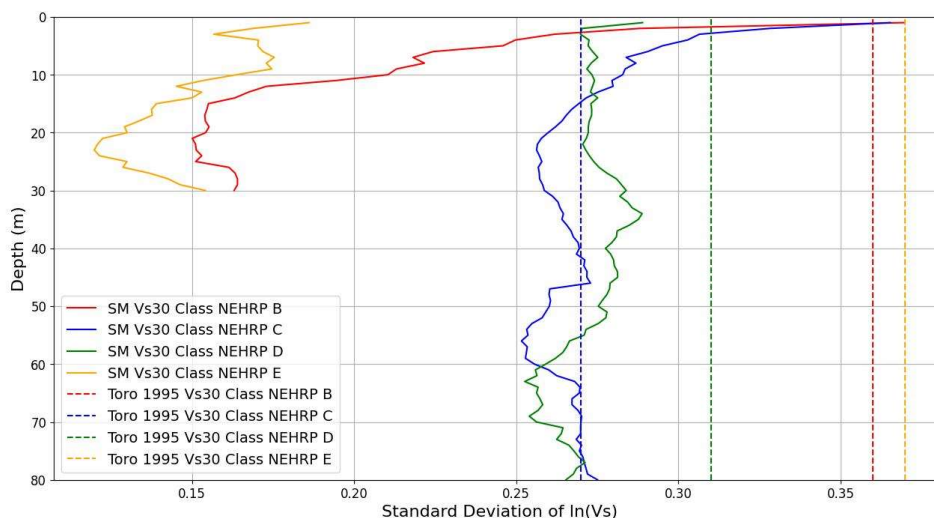


Figure 10: Results $\sigma \ln V_s$ by means of SM clustering (red lines; 25,50,75th percentile) and comparison with EPRI-SPID (1993) (green line) and Savannah river nuclear project (Toro, 1995; 1997) (purple line).



295

Figure 11: The $\sigma_{\ln V_s}$ values of V_s from our high-quality dataset, classified according to the 4 NEHRP soil categories; Toro (1995) constant $\sigma_{\ln V_s}$ values are also reported.

300

4 Data availability

The dataset is available at <https://doi.org/10.5281/zenodo.10885590> (Mori et al., 2024). The records are:

- survey id;
- survey latitude and longitude in UTM33N coordinates;
- survey type;
- depth in meters;
- shear wave velocity value (V_s) in m/s;
- seismic microzonation (SM) cluster id.

310

5 Conclusions

We analysed the largest dataset of shear wave velocity profiles (V_s) currently available, comprising approximately 15,000 profiles, with the aim of providing insight into the uncertainty of the shear wave velocity V_s ($\sigma_{\ln V_s}$) for each metre depth and



up to a maximum of 80 m. A first spatial analysis showed that the synthetic Vs data (Vs10, Vs20, Vs30) show nested
315 semivariograms with a first spherical model and a second exponential model: the first spatial structure shows a range of about
4,500 m, while the second structure shows a range of 25,000 m. A second spatial correlation analysis using Moran's index
revealed that the nature of the synthetic Vs data (Vs10, Vs20, Vs30) is inherently clustered, due to both the concentration of
data in urban areas and the discrete nature of the geological bodies. This result led us to investigate the logarithmic standard
deviation of the shear wave velocity ($\sigma_{\ln V_s}$) profiles in two different types of clusters: seismically homogeneous clusters based
320 on seismic microzones (SM), and non-seismically homogeneous clusters based only on geographic density (GC).

The variographic analysis allowed us to study $\sigma_{\ln V_s}$ by filtering high quality clusters, specifically by imposing a maximum
distance between surveys within clusters of 4,500 m, corresponding to the range value of the first spatial structure. The detailed
study of $\sigma_{\ln V_s}$ reveals the following significant statistical results:

- $\sigma_{\ln V_s}$ in clusters that are homogeneous in terms of expected seismic behaviour (i.e., based on Seismic Microzones,
325 SM) are consistently lower values than those obtained from geographic density clusters (GC); the difference is 14%
for the first 30 m, increasing to 2% at greater depths;
- $\sigma_{\ln V_s}$ values in guidelines for site-specific analyses (EPRI - SPID, 1993) are internal to the percentiles of the SM
statistics;
- $\sigma_{\ln V_s}$ values in clusters are lower than those previously reported in the literature for soil Vs30 classification,
330 indicating the effectiveness of our methodological approach, while confirming the effectiveness of seismic
microzonation as a tool for mapping in terms of expected site effects.

For practical applications, such as in numerical simulations to calculate seismic amplification, $\sigma_{\ln V_s}$ values are essential to
generate randomised velocity profiles. In this respect, our study supports the effective use of numerical simulation codes such
as STRATA (Kottke et al., 2013) and the recently developed NC92soil (Acunzo et al., 2024).

335 In addition, our results have broader implications for:

- optimising borehole sampling designs in seismic microzonation projects;
- improving seismic hazard analysis, in terms of better management of uncertainties arising from the use of the
parameter Vs.

Echoing Toro (2022), this study was inspired by the recommendation that "... *new site-specific stochastic Vs models should be*
340 *developed using these (recent) larger datasets, together with insights gained in research in the practical use of these models*".
This highlights the value of using large datasets and recent research results to develop stochastic Vs models that can be used
for site-specific applications and seismic hazard assessment.

Our contribution improves the discussion on seismic hazard calculation by addressing the complexities and uncertainties
associated with Vs in ground motion models. It is crucial to thoroughly control Vs-related uncertainties in site response
345 analysis, as they significantly affect the understanding of earthquake ground motions. Our conclusions highlight the importance
of paying close attention to uncertainties in seismic hazard assessment and contribute to the advancement the discipline in this
area.



Author contribution

350 F.M. Conceptualization / Methodology/ Formal analysis/ Writing; G.N. Conceptualization /Methodology/ Formal analysis/
Writing; A.M. Data curation /Writing; G.C. Formal analysis/ Writing; C.V. Formal analysis / Writing; M.M.
Conceptualization/ Supervision / Writing

Competing interests

355 The authors declare that they have no conflict of interest.

Acknowledgements

This work was supported by the Italian Department for Civil Protection of the Presidency of Council of Ministers within the
“Accordo ai sensi dell’art. 15 legge 7 agosto 1990, n. 241 tra la Presidenza del Consiglio dei Ministri il Dipartimento della
360 Protezione Civile e il Consiglio Nazionale delle Ricerche Istituto di Geologia Ambientale e Geoingegneria per il supporto al
Dipartimento della Protezione Civile per la realizzazione delle attività di cui all’ordinanza 780/2021 riguardanti gli interventi
di prevenzione del rischio sismico, previsti dall’art. 11 del decreto-legge 28 aprile 2009 n. 39, convertito, con modificazioni,
dalla legge 24 giugno 2009, n. 77, come rifinanziato dalla legge 30 dicembre 2018, n. 145 (CUP: B75F21002870001)” and
within the “Accordo ai sensi dell’art. 15 legge 7 agosto 1990, n. 241 tra la Presidenza del Consiglio dei Ministri il Dipartimento
365 della Protezione Civile e il Consiglio Nazionale delle Ricerche Istituto di Geologia Ambientale e Geoingegneria per il supporto
al Dipartimento della Protezione Civile per la programmazione degli interventi in materia di riduzione del rischio sismico ai
fini di protezione civile (CUP: B53C22009330001)”.

The activities of Amerigo Mendicelli were funded by “ICSC National Research Centre for High Performance Computing, Big
Data and Quantum Computing (CN00000013, CUP B93C22000620006) within the European Union-NextGenerationEU
370 program” (Scientific manager for CNR - IGAG: Massimiliano Moscatelli).

References

- Acunzo, G., Falcone, G., di Lernia, A., Mori, F., Mendicelli, A., Naso, G., Albarello, D. and Moscatelli, M. NC92Soil: A
computer code for deterministic and stochastic 1D equivalent linear seismic site response analyses. *Computers and*
375 *Geotechnics*, 165, 105857. doi: org/10.1016/j.compgeo.2023.105857, 2024.
- Chilès, J.-P., and Delfiner, P.: *Geostatistics: Modeling spatial uncertainty* (Vol. 497). John Wiley & Sons., 2009.
- Electric Power Research Institute (EPRI) (1993) *Guidelines for determining design basis ground motions, Volume 2:
Appendices for Ground Motion Estimation*. Palo Alto, CA. <https://www.epri.com/research/products/TR-102293-V2>. Accessed
March 2024.
- 380 Ester, M., Kriegel, H.-P., Sander, J., and Xu, X.: A density-based algorithm for discovering clusters in large spatial databases
with noise. *Proc. 2nd Int. Conf. on Knowledge Discovery and Data Mining*. Portland, OR, pp. 226–231, 1996.



- Falcone, G., Acunzo, G., Mendicelli, A., Mori, F., Naso, G., Peronace, E., Porchia, A., Romagnoli, G., Tarquini, E. and Moscatelli, M.: Seismic amplification maps of Italy based on site-specific microzonation dataset and one-dimensional numerical approach. *Engineering Geology*, 289, 106170. doi: [org/10.1016/j.enggeo.2021.106170](https://doi.org/10.1016/j.enggeo.2021.106170), 2021.
- 385 Gaudiosi, I., Romagnoli, G., Albarello, D., Fortunato, C., Imprescia, P., Stigliano, F. and Moscatelli, M.: Shear modulus reduction and damping ratios curves joined with engineering geological units in Italy. *Scientific Data*, 10(1). doi: [org/10.1038/s41597-023-02412-8](https://doi.org/10.1038/s41597-023-02412-8), 2023.
- Goovaerts, P.: *Geostatistics for Natural Resources Evaluation*, 477 pp., Oxford Univ. Press, New York, 1997.
- Isaaks, E. H., and Mohan Srivastava, R.: *An Introduction to Applied Geostatistics*, 561 pp., Oxford Univ. Press, New York, 390 1989.
- Journel, A. G.: *Geostatistics for the environmental sciences*, EPA Proj. Rep. CR 811893, Environ. Protect. Agency, Environ. Monit. Syst. Lab., Las Vegas, Nev, 1987.
- Journel, A. G., and Huijbregts, Ch. J.: *Mining geostatistics*. Blackburn Press. 1978.
- Kottke, A., Wang, X., Rathje, E.M.: *Technical Manual for STRATA*. Rep. No. 2008/10. Pacific Earthquake Engineering Research Center, Berkeley, CA, USA, 2013.
- 395 Krige, D. G.: Two-dimensional weighted moving average trend surfaces for ore-evaluation, *J. S. Afr. Inst. Min. Metall.*, 66, 13–38, 1966.
- Matheron, G.: *The theory of regionalized variables and its applications*, Cah. 5, Centre de Morphol. Math., Fontainebleau, France, 1971.
- 400 McInnes, L., Healy, J., and Astels, S.: hdbscan: hierarchical density based clustering. *The Journal of Open Source Software*. 2. 10.21105/joss.00205, 2017.
- Moscatelli, M., Albarello, D., Scarascia Mugnozza, G. and Dolce, M.: The Italian approach to seismic microzonation, *Bull. Earthq. Eng.*, <https://doi.org/10.1007/s10518-020-00856-6>, 2020.
- Moran, P.A.P.: Notes on Continuous Stochastic Phenomena. *Biometrik* 37 (1/2): 17–23.
- 405 <https://doi.org/https://doi.org/10.2307/2332142>, 1950
- Mori, F., Mendicelli, A., Moscatelli, M., Romagnoli, G., Peronace, E. and Naso, G.: A new Vs30 map for Italy based on the seismic microzonation dataset. *Engineering Geology*, 275, 105745. doi: [org/10.1016/j.enggeo.2020.105745](https://doi.org/10.1016/j.enggeo.2020.105745), 2020.
- Mori, F., Mendicelli, A., Moscatelli, M., & Varone, C. (2024). Shear wave velocity profiles from Italian Seismic Microzonation project [Data set]. Zenodo. <https://doi.org/10.5281/zenodo.10885590>
- 410 Romagnoli, G., Tarquini, E., Porchia A., Catalano, S., Albarello, D. and Moscatelli, M.: Constraints for the Vs profiles from engineering-geological qualitative characterization of shallow subsoil in seismic microzonation studies *Soil Dyn. Earthq. Eng.*, 161, Article 107347, doi: [10.1016/J.SOILDYN.2022.107347](https://doi.org/10.1016/J.SOILDYN.2022.107347), 2022.
- Shi, J. and Asimaki, D.: A generic velocity profile for basin sediments in California conditioned on VS30. *Seismol Res Lett* 415 89:1397–1409, 2018.



- Seismic Microzonation Working Group: Indirizzi e criteri per la microzonazione sismica – Guidelines for seismic microzonation. Conferenza delle Regioni e delle Province Autonome - Dipartimento della Protezione Civile. Available at www.protezionecivile.gov.it/httpdocs/cms/attach_extra/GuidelinesForSeismicMicrozonation.pdf, 2008.
- Stewart, J.P., Afshari, K. and Hashash, Y.M.: Guidelines for performing hazard-consistent one-dimensional ground response analysis for ground motion prediction. PEER Report, 2014/16, 2014.
- 420 Toro, G.R.: Probabilistic models of the site velocity profiles for generic and site-specific ground-motion amplification studies. Appendix in Technical Rep. No. 779574, Brookhaven National Laboratory, Upton, NY, 1995.
- Toro, G.R.: Probabilistic models of site velocity profiles at the Savannah River Site, Aiken, South Carolina. Report by Risk Engineering, Inc. for Pacific Engineering and Analysis. Published as an appendix in Lee, R.C.; Maryak, M.E.; and McHood, M.D. 1997. SRS Seismic Response Analysis and Design Basis Guidelines. WSRC-TR-97-0085, Rev. 0. Aiken, South Carolina: Westinghouse Savannah River Company. <https://doi.org/10.13140/RG.2.2.20590.69447>, 1997.
- 425 Toro, G.R.: Uncertainty in Shear-Wave Velocity Profiles. *J Seismol*, 26, 713–730. doi.org/10.1007/s10950-022-10084-x, 2022.
- Varone, C., Carbone, G., Baris, A., Caciolli, A.C., Fabozzi, S., Fortunato, C., Gaudiosi, I., Giallini, S., Mancini, M., Paoletta, L., Simionato, M., Sirianni, P., Spacagna, R.L., Stigliano, F., Tentori, D., Martelli, L., Modoni, G. and Moscatelli, M.: PERL: A dataset of geotechnical, geophysical, and hydrogeological parameters for earthquake-induced hazards assessment in Terre del Reno (Emilia-Romagna, Italy), 23, 1371-1382, 2023. <https://doi.org/10.5194/nhess-23-1371-2023>.
- 430 Zhou J., Li L., Li X., Yu Y., Tian Q. Lateral variations of shear wave velocity (VS) profile and VS30 over gentle terrain. *Soil Dynamics and Earthquake Engineering*, 175, 18265. doi.org/10.1016/j.soildyn.2023.108265, 2023.